SIMULATION OF LAMINAR FORCED CONVECTION HEAT TRANSFER AND FLUID FLOW OVER A BACKWARD FACING STEP WITH OBSTACLE USING (SIO_2) NANOPARTICLES

Mohammed Saad Kamel **Ahmed Khafeef Obaid Albdoor**

Southern Technical University/ Al-Nassiriyah Technical Institute Department of Mechanical Techniques

Mr.mohd1986@yahoo.com **Ahmedalbadry82@yahoo.com**

***Abstract*:** Simulation of Heat transfer and laminar Sio_2/water and Sio_2/oil-engine flow over backward facing step with and without obstacle numerically studied in this paper. The finite volume method adopted to solve continuity, momentum and energy equations in two dimensions. The aspect ratio of triangular obstacle *w/e* = 0.5 presented. The step height and expansion ratio of channel were 4.8_{mm} and 2 respectively, the range of Reynolds number varied from 100 to 250, constant heat flux subjected on downstream of wall was $2000W/m^2$.Two types of base fluid used in this simulation the water and oil-engine with constant properties at T = 300K°, The Sio_2 nanoparticles used with nanoparticles diameter 30*nm* and volume friction 4%. The average nusselt number noticed increase with increase Reynolds number with obstacle for two basefluid and also noticed that the nanofluid of Sio_2-oil engine has higher nusselt number compared with other nonofluid. The result shows increase of local nusselt number for backward facing step with obstacle in compared to those without obstacle. The maximum enhancement of heat transfer observed at obstacle due to increase recirculation flow after the obstacle. Streamline showing the increase of recirculation region with used obstacle in compared without obstacle and highest recirculation region observed at obstacle.

Keywords: laminar flow, backward facing step, Sio_2 nanoparticles, forced convection.

المستخلص : محاكاة انتقال الحرارة و الجريان الطباقي للماء مع Sio2 و زيت المحرك مع SiO_2 فوق عتبة موجهة للخلف مع و بدون عائق تم دراستها عددياً في هذه الدراسة . تم اعتماد طريقة الحجوم المحددة لحل معادلات الاستمرارية ، الزخم و الطاقة في بعدين . اعتمدت نسبة العرض الى الارتفاع للعائق المثلث (w/e = 0.5) . وكان ارتفاع العتبة و نسبة توسع القناة mm 4.8 و 2 على التوالي . مدى اعداد رينولدز اختلف من 100 الى 250 . فيض حراري ثابت عرض له الجريان بعد الجدار وكانت قيمته $2000W/m^2$ في هذه . نوعين من الموائع الأساسية استخدمت المحاكاة الماء و زيت المحرك بخصائص ثابتة عند درجة حرارة K ° T = 300 . جزيئات Sio2 استخدمت بقطر جزيئات نانوية nm 30% . عدد نسلت المعدل لوحظ انه يزداد مع زيادة عدد رينولدز بوجود العائق 4 و حجم احتكاك للمائعين الأساسيين الأثنين و يلاحظ أيضاً ان المائع النانوي SiO_2 مع زيت المحرك يمتلك اعلى قيم لأعداد نسلت بالمقارنة مع المائع النانوي الاخر . النتائج بينت زيادة في قيم اعداد نسلت الموقعية للعتبة الموجهة للخلف بوجود العائق بالمقارنة معها بدون عائق . اقصى تحسين في انتقال الحرارة لوحظ في العقبة بسبب زيادة إعادة تدوير الجريان بعد العائق . خطوط الانسياب بينت زيادة في منطقة اعادة التدوير باستخدام العائق بالمقارنة مع بدون العائق وان اكبر منطقة اعادة تدوير لوحظت في العائق .

1- Introduction:

Flow over a backward facing step generates recirculation zone and forms vortices due to the separation flow obtained from the adverse pressure gradients in fluid flow. Improve thermal performance in different engineering application become main goal in recent presented researches as the fluid flow over backward facing step is common geometry used in cooling and heating systems such as heat exchangers, chemical process, power plants, and nuclear

reactor due to generate separation and reattachment region. In addition, used obstacle in flow passage leads to increase of static pressure and then enhance of heat transfer [1]. Many researcher have been studied an experimental and numerical for analysis heat transfer and fluid flow over backward facing step. Armaly et al. [2] have experimental and numerical studied of laminar, transition, and turbulent air flow over backward-facing step. They found that the separation length increase with increase of the Reynolds number for Re< 1200 while reduction at Re between 1200 to 5550. De Zilwa et al. [3] developed new calculation method for study laminar and turbulent flows through plane sudden expansions. The calculations of laminar range found that increase thickness of the separating up to reach bigger separation region and used k- ε models for turbulent range as obtained good agreement compared to experimental results. Effect of step height on non-Newtonian liquids flow through sudden expansion investigated by Pak et al. [4] where found that decrease of length reattachment at non-Newtonian liquid compared to water for same boundary condition of flow. Khanafer et al. [5] performed numerical study of heat transfer to laminar mixed convection of pulsatile flow over a backward-facing step by using finite element method. They showed that improve of the heat transfer rate with increased of Reynolds number but the thickness of the thermal boundary layer reduced. two-phase flow over backward-facing step with low and high Reynolds number numerically studied by Yu et al. [6] in 2D and 3D dimension. LES was applied and found good agreement between 2D-3D numerical result with experimental result in profile of velocity and temperature distribution. Heat transfer to laminar fluid flow between parallel plates through baffles was numerically studied by Kelkar and Patankar [7]. The study described flow by strong deformations and large recirculation regions and found increase of Nusselt number and friction coefficient with increased Reynolds number.

More recently, the majority of studies have been utilizing nanofluid because of its higher thermal conductivity compared to normal fluid [8]. Abu Nada [9] is a pioneer in research on laminar nanofluid flow over a backward-facing step with Cu, Ag, Al_2O_3, CuO, and TiO_2 nanofluid, volume fractions between 0.05 and 0.2 and Reynolds numbers ranging from 200 to 600. An investigation of findings signifies that the Nusselt number increased with the volume fraction and Reynolds number. Later, Kherbeet et al. [10] presented a numerical investigation of heat transfer and laminar nanofluid flow over a micro-scale backward-facing step. The Reynolds numbers ranged from 0.01 to 0.5, nanoparticle types comprised Al2O3, CuO, SiO_2, and ZnO, and the expansion ratio was 2. An increasing Reynolds number and volume fraction seemed to lead to an increasing Nusselt number; the highest Nusselt number value was obtained with SiO2. Additional last investigations concern nanofluid flow over a backward-facing step for the laminar range [11–12], but such work with respect to the turbulent regime, in particular, is still not entirely understood. Due to the Cu has higher thermal conductivity and many experimental investigations done with good improvement in thermal performance then used in this simulation.

The aim of the present work is to investigate the heat transfer and laminar fluid flow over backward facing step with and without obstacle by using two types of basefluid with Sio2 nanoparticles. The numerical data for used obstacle in flow passage with backward facing step will be more helpful to design thermal channel with higher performance. In this investigation, Finite Volume Method in commercial program FLUENT 6.3.26 is employed.

2- Numerical model

2.1 Description of geometry

In this simulation, the geometry and flow domain is shown in Fig. 1 where the dimension of geometry was according to Al-Aswadi et al. [12]. Backward-facing step of duct with and without triangular obstacle are adopted. The height of obstacle is 4mm and 2mm width fixed at 200mm from the step with expansion ratio 2 at Reynolds numbers of 100, 175, and 250.

The total length of duct is 1050mm consist of 50mm upstream length and 1000mm downstream length and inlet height of duct is 4.8mm and exit height is 9.6mm. Constant heat flux (2000 W/m^2) is subjected on downward of duct while insulated other parts of duct. Two working fluids used as a basefluid pure water and oil-engine and then added Sio_2 nanoparticles for them at constant volume friction and constant diameter of nanoparticles (4% and 30nm respectively) to study the enhancement of heat transfer with and without obstacle.

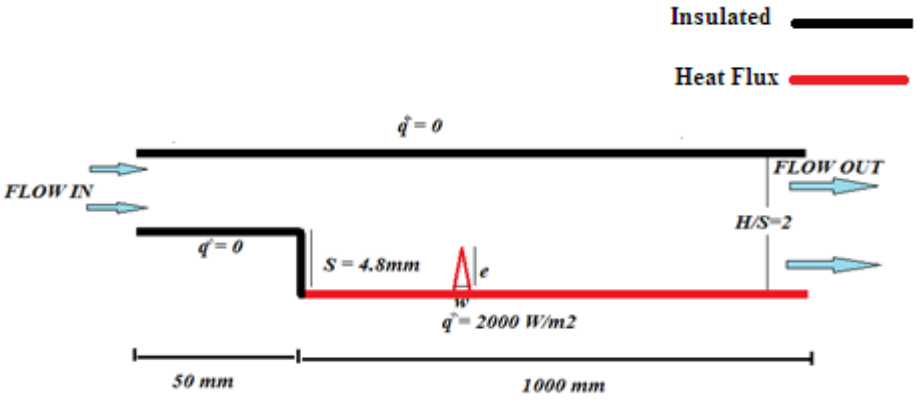

Figure 1. Geometry domain and boundary condition

2.2 Governing Equations:

Continuity, momentum (X, Y) and energy equations with assumption laminar, steady state, incompressible, and two dimensional are employed in this simulation and can be written as (1)-(4).

$$\frac{\partial u}{\partial x}+\frac{\partial v}{\partial y}=0 \qquad \text{.....(1)}$$

$$u\frac{\partial u}{\partial x}+v\frac{\partial u}{\partial y}=-\frac{1}{\rho}\frac{\partial p}{\partial x}+\nu\left(\frac{\partial^2 u}{\partial x^2}+\frac{\partial^2 u}{\partial y^2}\right) \qquad \text{.....(2)}$$

$$u\frac{\partial v}{\partial x}+v\frac{\partial v}{\partial y}=-\frac{1}{\rho}\frac{\partial p}{\partial y}+\nu\left(\frac{\partial^2 v}{\partial x^2}+\frac{\partial^2 v}{\partial y^2}\right) \qquad \text{.....(3)}$$

$$u\frac{\partial T}{\partial x}+v\frac{\partial T}{\partial y}=-\frac{1}{\rho}\frac{\partial p}{\partial y}+\alpha\left(\frac{\partial^2 T}{\partial x^2}+\frac{\partial^2 T}{\partial y^2}\right) \qquad \text{.....(4)}$$

Where u and v represent velocities in x, y direction respectively, ρ and α define density and thermal expansion, respectively.

The Reynolds number is computed based on inlet channel height (H).

$$Re=\frac{\rho u H}{\mu} \qquad \text{.....(5)}$$

$$Nu_{av}=\frac{1}{L}\int_0^L Nu_L\ dL \qquad \text{.....(6)}$$

Where (L) is the length of the heated downstream wall.

2.3 Boundary conditions

The boundary conditions for this simulation are:

- At the inlet Chanel the fluid is assumed to enter with a uniform horizontal velocity U∞ and temperature (T∞) U=U∞, T=T∞=300K, V=0;
- At the outlet Chanel: P=0,
- Insulated top wall of the of duct. The mathematical form of this condition: $\frac{\partial U}{\partial y}$ =0, V=0, $q^{"}$= 0
- For the downward of duct Constant heat flux $q^{"}$ (2000 W/m^2) is subjected while insulated other parts of duct

2.4 Numerical procedure and Data Validation

FLUENT 6.3.26 software with computational fluid dynamics (CFD) were conducted in numerical simulations. The procedure for generate geometry and meshing process was performed with Gambit 2.3.16 software. Viscous laminar flow model with energy dialog box was selected to solve continuity and X,Y momentum equations as well as energy equation. In computational fluid dynamics (CFD), SIMPLE algorithm is a commonly used in numerical procedure to solve the Navier-Stokes equations therefore employed to link the velocity and pressure fields. The residual of solution was smaller than (10^{-4}) for continuity equation, (10^{-5}) for momentum equations and (10^{-6}) for energy equation. In order to increase accuracy of solution, the density of mesh at backward and obstacle was more highly than other parts. The computational conditions and thermo-physical properties used in the numerical simulation are shown in Table 1. Five size of grid was adopted at Re =175 and airflow as a working fluid. Where the grid densities was (19558, 40864, 70752, 116506 and 228700) triangular cells. The grid independent selected (116506) cells among the others due to the difference in nusselt number was less than 3% compared to the grids as shown in Figure. 2. For purpose of validations used boundary conditions as reported by Al-Aswadi et al. [12] and then obtained results with acceptable agreement as shown in Figure. 3.

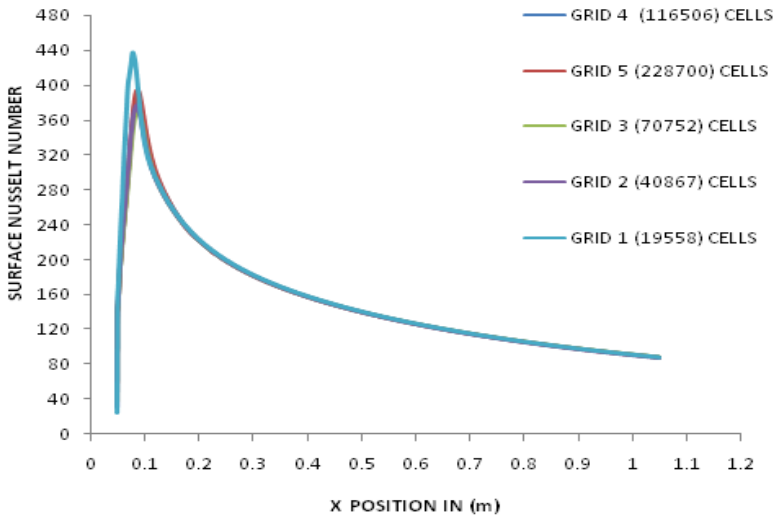

Figure 2. Grid independence test results for the Nusselt number

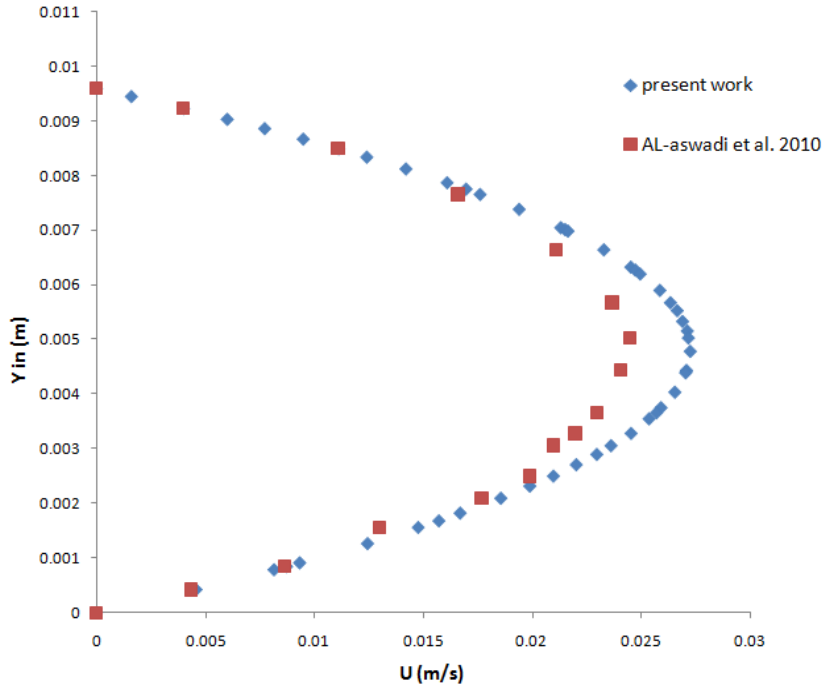

Figure 3. Comparison velocity profile with Al-Aswadi et al. [12].

Table 1. The computational conditions and thermo-physical properties

COMPUTATIONAL CONDITIONS		***[13]**	***[14]**
Fluid	Water (basefluid)	Oil-engine (basefluid)	Sio_2 nanoparticles
Pressure velocity coupling scheme	SIMPLE	SIMPLE	SIMPLE
Density	998.2 kg/m^3	884.1 kg/m^3 *	2220 kg/m^3 *
Viscosity	0.001 (N.s/m^3)	0.486 (N.s/m^3) *	-
Thermal conductivity	0.6 (W/m.K)	0.145 (W/m.K) *	1.4 (W/m.K) *
Heat capacity	4182 (J/Kg.K)	1909 (J/Kg.K) *	745 (J/Kg.K) *
Viscous model	Laminar model	Laminar model	Laminar model
Reynolds number	100, 175 and 250	100, 175 and 250	100, 175 and 250
Thermal heat flux	2000 W/m^2	2000 W/m^2	2000 W/m^2

3- Thermo-physical properties of nanofluids:

The effective properties of nanofluid are defined as follow:

Density:

$$\rho_{nf} = \varphi\rho_p + (1-\varphi)\rho_{bf} \quad \text{.....(7)}$$

Heat capacity:

$$cp_{nf} = \frac{\varphi\rho_p cp_p + (1-\varphi)\rho_{bf} cp_{bf}}{\rho_{nf}} \quad \text{.....(8)}$$

The Eqs. (6) and (7) were introduced by [15].

The thermal conductivity:

$$\frac{K_{nf}}{K_{bf}} = \frac{K_p + (n-1)K_{bf} - (n-1)\varphi(K_{bf} - K_p)}{K_p + (n-1)K_{bf} + \varphi(K_{bf} - K_p)} \quad \text{.....(9)}$$

This was introduced by [16].

Where (n) is a shape factor and equal to (3) for spherical nanoparticles.
The viscosity:

The effective viscosity can be obtained by using the following mean empirical correlation [17].

$$\mu_{nf} = \mu_{bf} \frac{1}{(1-34.87(d_p/d_{bf})^{-0.3}\,\varphi^{1.03})} \quad \text{.....(10)}$$

Where: $d_{bf} = \left[\frac{6M}{N\pi\rho_{bf}}\right]^{1/3}$ .....(11)

Where: M is the molecular weight of basefluid, N is the Avogadro number = $6.022*10^{23}$ mol^{-1}, ρ_{bf} is the mass density of the basefluid calculated at temperature T_0=300 K. the table 1. Show the thermo-physical properties of nanoparticles and working fluids.

4- Results and discussion:

4.1 The effect of different base fluids

The effect of two types of base fluids on the Nusselt number versus the Reynolds number is presented in Fig.5. It can clearly be seen that Sio_2–oil engine has the highest value of Nusselt number while Sio_2–water has the lowest value of Nusselt number. This is because oil engine has the highest dynamic viscosity in nature compared to other base fluids and Sio_2 particles

are mixed properly in oil engine which contributes to increase the thermal transport capacity of the mixture which in turn increases the Nusselt number.

4.2 The effect of the Reynolds number

The effects of the Reynolds number on the local nusselt number for the laminar ranges with and without obstacle are presented in Figures. 4(A),(B) respectively. With the increase of Reynolds number, the nusselt number increased in the laminar ranges. Effect of Reynolds number on surface nusselt number with axial distance at case with and without obstacle is illustrated. Generally, increase of surface nusselt number found with increase Reynolds number for all cases which denote to enhancement of thermal performance.

4.3 Average Nusselt number

In Figure. 5 the variation of average Nusselt number with the Reynolds number at different nanofluid with and without obstacle can be seen. For all cases, the average Nusselt number augmented as the Reynolds number increased. The highest Nusselt number was obtained at 250 Reynolds number. The maximum ratio of enhancement heat transfer to nanofluid was about ٣٤% for Sio_2-oil engine with obstacle compared with Sio_2-water with obstacle due to increase of intensity convection of enhanced conductivity nanofluid.

4.4 Streamline of Velocity

Streamline of velocity for backward facing step with and without obstacle for both nanofluids at Reynolds number 250 are illustrated in Figure. 6. It can be seen that the recirculation region is clearly appeared at the inlet region of backward and after obstacle due to pressure gradient. Increase size of recirculation region found with increase Reynolds number as shown in Figure. 7. Where the largest region noticed at Reynolds number 250 with obstacle and Sio_2-oil engine compared with other cases.

4.5 pressure drop

The pressure drop variation with axial distance for different Reynolds numbers and Sio_2-water nanofluids is presented in Figures. 6 and 7. According to the results, the pressure drop intensified as the Reynolds number increased and nanofluid volume fraction. Generally, the highest pressure drop occurred at the downstream inlet region with obstacle due to recirculation flow which caused the improvement of heat transfer.

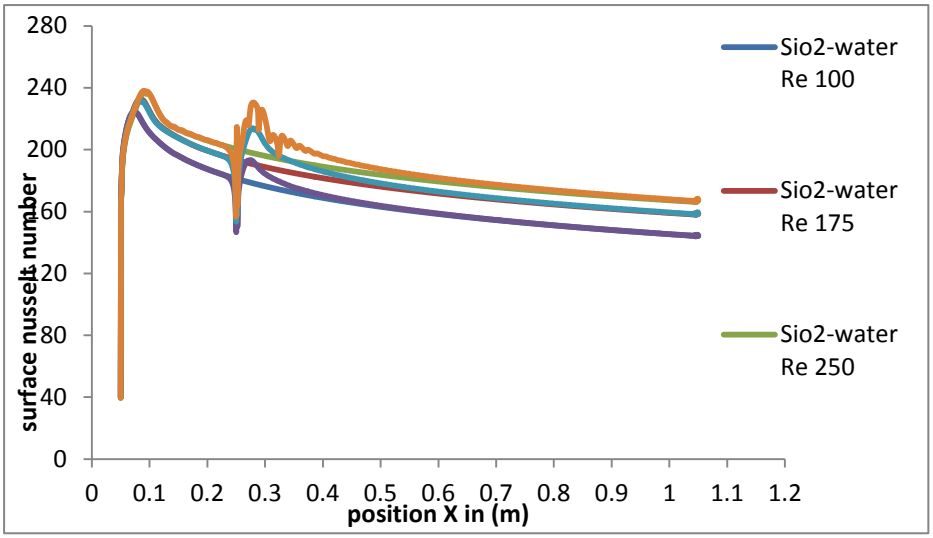

(A)

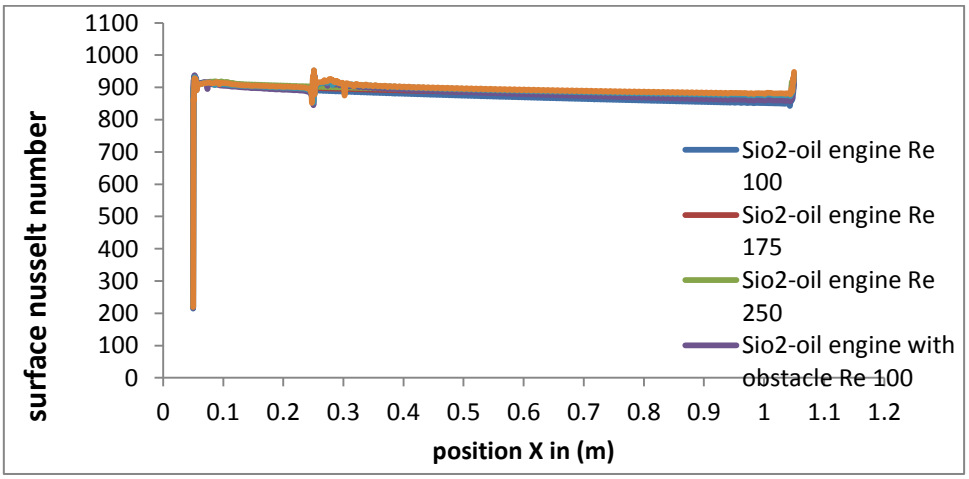

(B)

Figure 4. Surface nusselt number with x position at different Reynolds number (A) for Sio2-water with and without obstacle (B) for Sio2-oil engine with and without obstacle

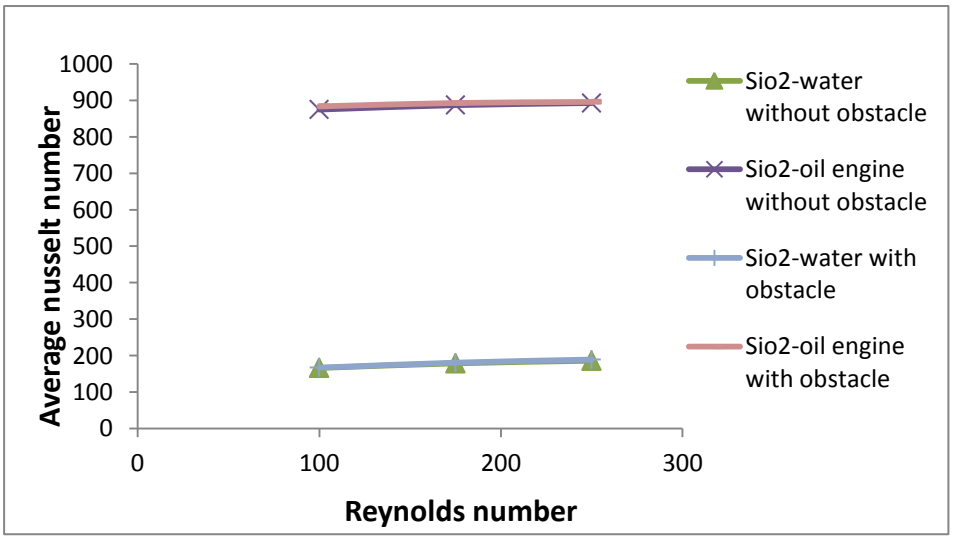

Figure 5. Average Nussult with Reynolds number

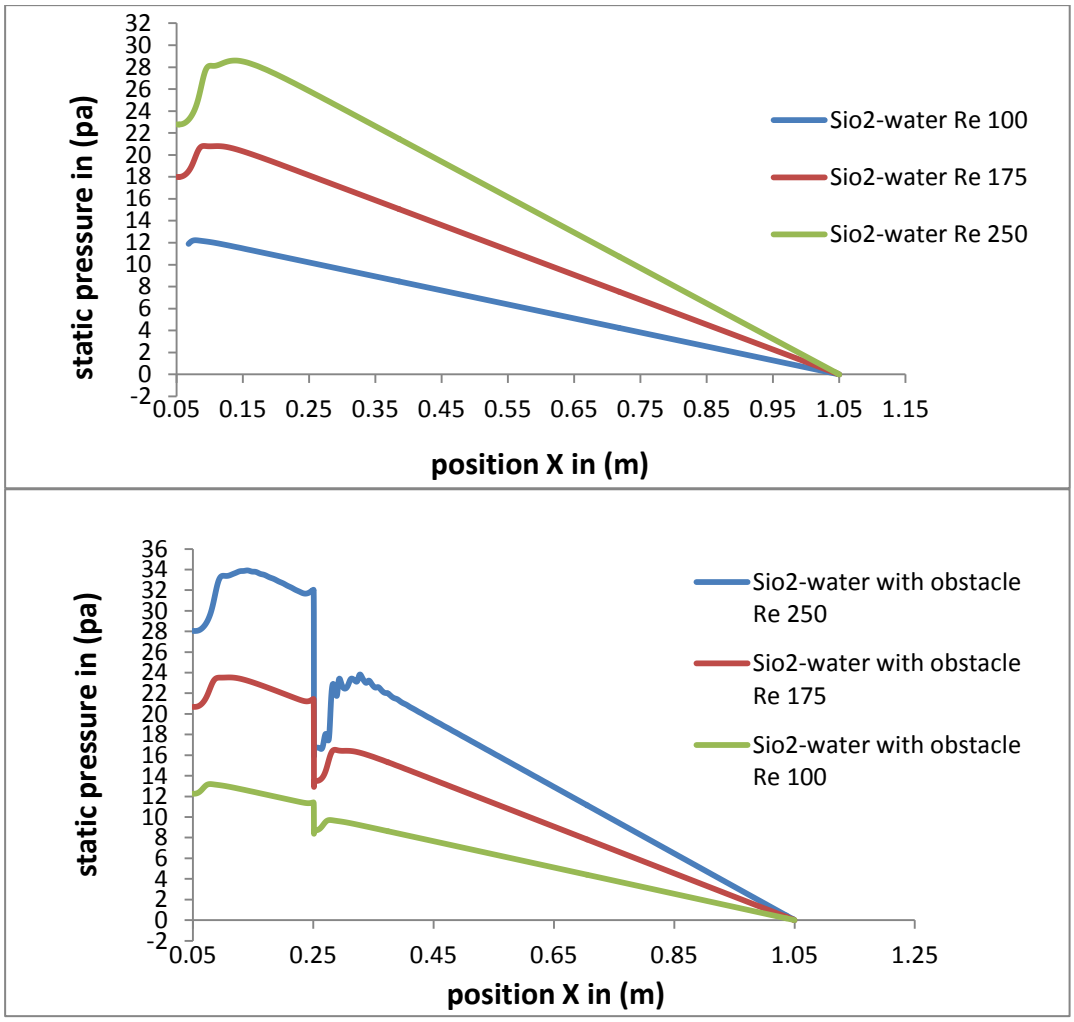

Figure 6. Statics pressure with different Reynolds number for Sio2-water with and without obstacle

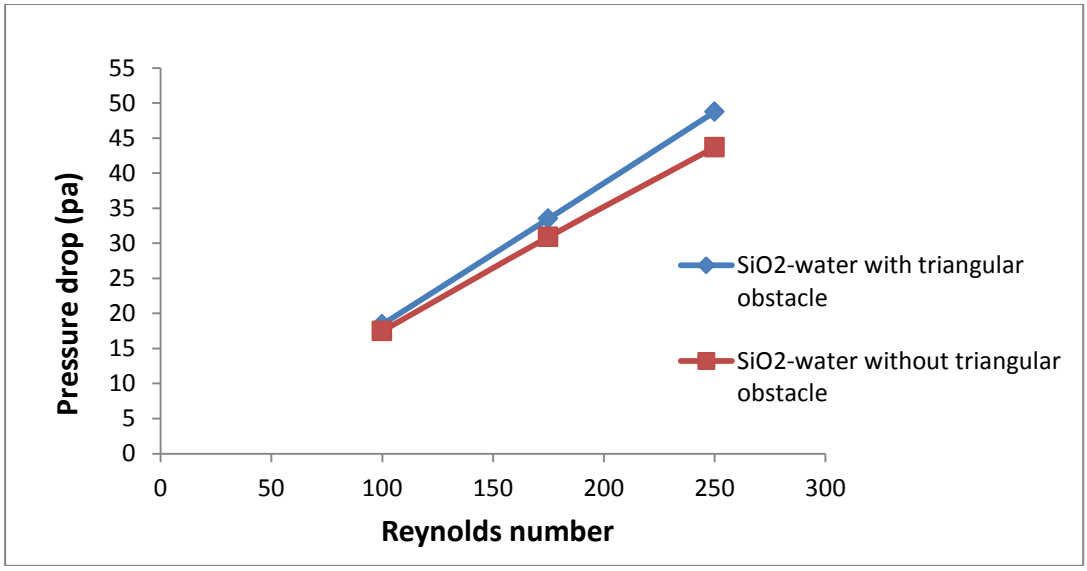

Figure 7. Pressure drop with different Reynolds number for Sio2-water with and without

obstacle

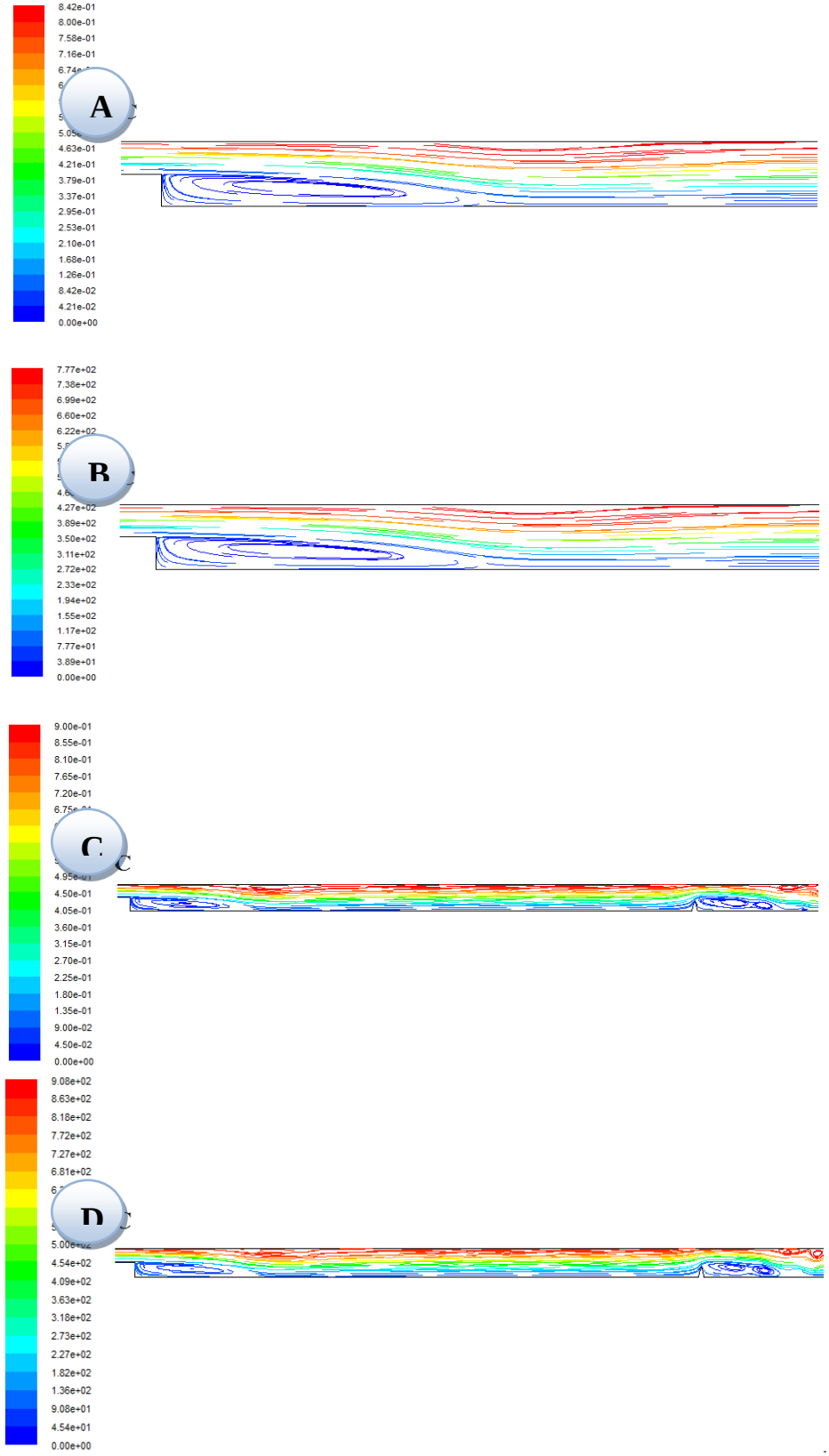

Figure 6. Velocity streamline at expansion ratio 2 without obstacle for (A) Sio2-water flow, (B) Sio2-oil engine flow (C) Sio2-water with obstacle , (D) Sio2-oil engine with obstacle at Re 250.

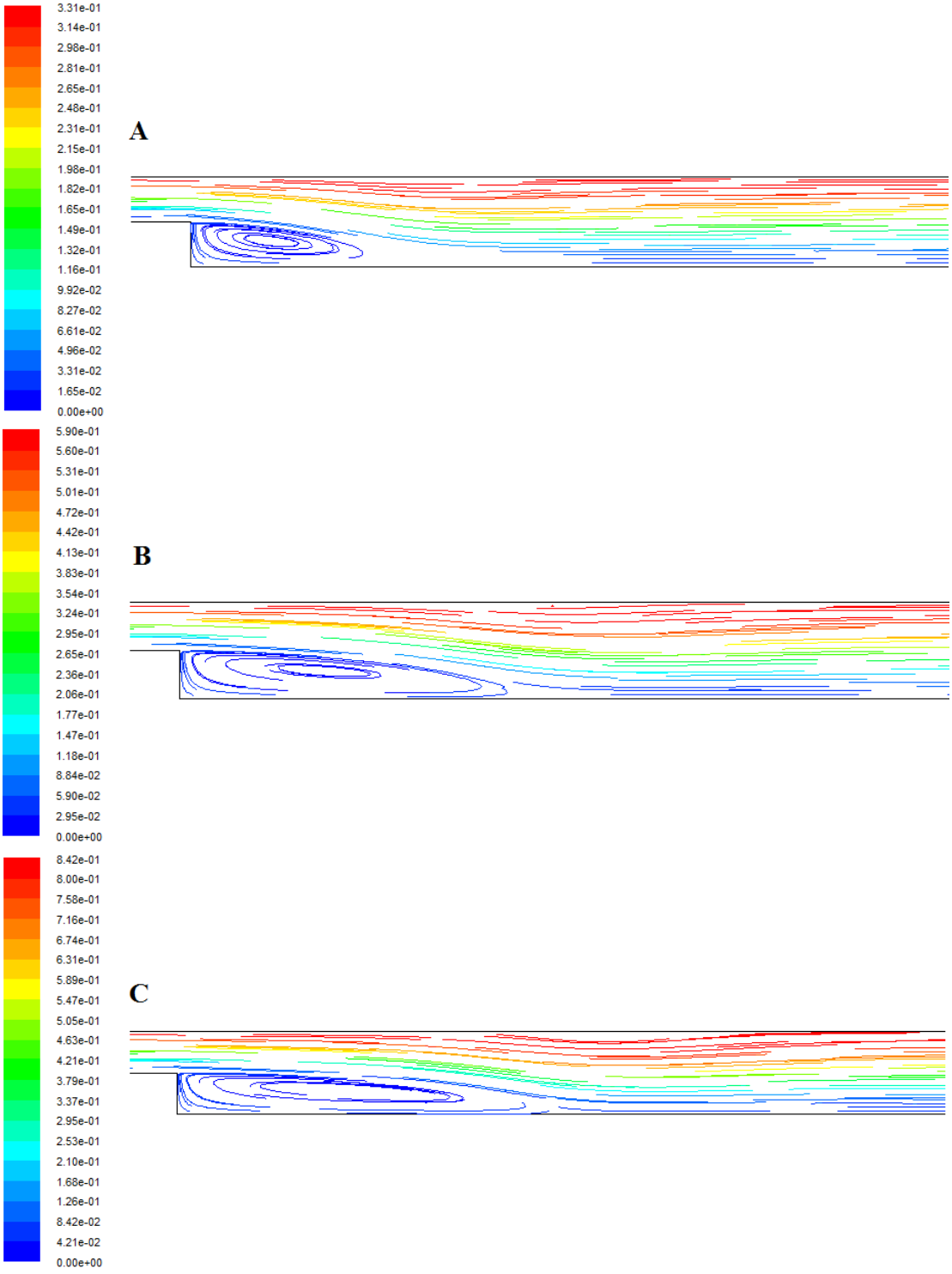

Figure 7. Velocity streamline at expansion ratio 2 without obstacle for Sio2-water
At Re A. 100 B. 175 C. 250

Nomenclature:

Cp	specific heat capacity (J kg^{-1} K^{-1})
Nu_L	surface Nusselt number
Nu_{av}	average Nusselt number
P	Pressure (Pa)
Pr	Prandtl number
q	heat flux (W m^{-2})
Re	Reynolds number
T	temperature (K)
u	velocity component (m s^{-1})
x, y	spatial coordination (m)
L	Length of the heated downstream wall (m)
S	Step height
H	Height of outlet channel (m)
h	Height of inlet channel (m)
e	Height of obstacle (m)
w	Width of obstacle (m)
M	molecular weight of basefluid
d_p	Particles diameter (nm)
d_{bf}	Basefluid diameter (nm)
N	Avogadro number

Greek symbols

K	thermal conductivity (W m^{-1} K^{-1})
μ	dynamic viscosity (Pa s)
ρ	density (kg m^{-3})
α	Thermal expansion
ρ_{bf}	Density of basefluid (kg m^{-3})
φ	Volume friction (%)

Subscripts

nf	nanofluid
p	Nano particles
bf	basefluid

References:

[1] Hussein Togun, Tuqa Abdulrazzaq, S. N. Kazi, A. Badarudin, M. K. A. Ariffin, M. N. M. Zubir "Numerical Study of Heat Transfer and Laminar Flow over a Backward Facing Step with and without Obstacle " "International Journal of Mechanical, Aerospace, Industrial and Mechatronics Engineering" Vol:8 No:2, 2014. **[2]** B.F. Armaly, F. Durst, J.C.F. Pereira, B. Schonung, "Experimental and theoretical investigation of backward-facing step flow," Journal of Fluid Mechanics, vol.127, pp. 473-496, 1983.

[3] De Zilwa, S .R N., Khezzar, L. K. and Whitelaw, J. H., "Flows through plane sudden-expansions", International Journal for Numerical Methods in Fluids, vol. 32, pp. 313-329, 2000.
[4] B. Pak, Y.I. Cho, S.U.S. Choi, "Separation and reattachment of nonnewtonian fluid flows in a sudden expansion pipe, "Journal of Non- Newtonian Fluid Mechanics, vol. 37, pp. 175-199, 1990.
[5] K. Khanafer, B. Al-Azmi, A. Al-Shammari, I. Pop, "Mixed convection analysis of laminar pulsating flow and heat transfer over a backward facing step, International Journal of Heat and Mass Transfer, vol. 51, pp. 5785-5793, 2008.
[6] K. F. Yu, Eric W. M. Lee, Jason K.K. Yuen, "High and low Reynolds number two-phase flows over a backward-facing step by 2D and 3D large eddy simulation," International Journal of Nonlinear Sciences and Numerical Simulation. Vol.10, no. 9, pp. 1135-1158, 2011.
[7] K. M. Kelkar, S. V. Patankar, "Numerical prediction of flow and heat transfer in a parallel plate channel with staggered fins", Journal of Heat Transfer, vol. 109, pp.25-30, 1987.
[8] M. Hassan, R. Sadri, G. Ahmadi, M. Dahari, S. Kazi, M.R. Safaei, E. Sadeghinezhad, Numerical study of entropy generation in a flowing nanofluid used in micro- and minichannels, Entropy 15 (2013) 144–155.
[9] E. Abu-Nada, Application of nanofluids for heat transfer enhancement of separated flows encountered in a backward facing step, Int. J. Heat Fluid Flow 29 (2008) 242–249.
[10] A.S. Kherbeet, H.A. Mohammed, B.H. Salman, The effect of nanofluids flow on mixed convection heat transfer over microscale backward-facing step, Int. J. Heat Mass Transfer 55 (2012) 5870–5881.
[11] H.A. Mohammed, A.A. Al-Aswadi, H.I. Abu-Mulaweh, A.K. Hussein, P.R. Kanna, Mixed convection over a backward-facing step in a vertical duct using Nanofluids-buoyancy opposing case, J. Comput. Theor. Nanosci. 11 (2014) 860–872.
[12] A.A. Al-aswadi, H.A. Mohammed, N.H. Shuaib, A. Campo, "Laminar forced convection flow over a backward facing step using nanofluids" International Communications in Heat and Mass Transfer, vol. 37, no.8, pp. 950-957, 2010.
[13] F.P Incropera, D.P Dewitt, T.L. Bergma, A.S. Lavine, fundamentals of heat and mass transfer, 6th edition Wiley, 2007.
[14] I.V. Lienhard, V. Lienhard, A heat transfer Textbook, third edition phlogiston press, 2006.
[15] Buongiorno J (2006) Convective transport in nanofluids. ASME J. Heat Transfer. 128, 240‑250.
[16] Hamilton RL and Crosser OK (1962) Thermal conductivity of heterogeneous two component systems. I&EC Fundamen. 1,187‑191.
[17] M. Corcione, heat transfer features of buoyancy-driven nanofluids inside rectangular enclosures differentially heated at the sidewalls, international journal of thermal sciences 49 (2010) 1536-1546.